Journal of Ovonic Research Vol. 14, No. 4, July - August 2018, p. 269 - 275

PHOTODEGRADATION ACTIVITY OF PURE, PVP CAPPED AND CHITOSAN CAPPED ZnO NANOPARTICLES AGAINST AZO RED DYE UNDER UV IRRADIATION

V. JEEVANANTHAM[a*], K. V. HEMALATHA[b], S. SATHEESKUMAR[c]
[a]*Assistant Professor, Department of Chemistry, Rathinam Institute of Technology, Coimbatore - 641021 Tamil Nadu, India*
[b]*Assistant Professor, Department of Chemistry, Coimbatore Institute of Technology,*
Coimbatore-641014, Tamilnadu, India.
[c]*Assistant Professor, Department of Physics, KSR Institute for Engineering and Technology, Tiruchengode- 637215, Tamilnadu, India.*

ZnO NPs of different surface morphologies are synthesized by different methods. These II-IV group metal oxide semiconductor photocatalysts are potentially explored photodegradation of Azo red dye in water. The structural and optical properties of synthesized nanoparticles were analyzed using XRD, SEM, UV and PL techniques. The results showed that the average particle size of the prepared nanoparticles was 15 nm – 20 nm. The photodegradation effects against azo red dye investigated by pure, PVP and Chitosan capped ZnO nanoparticles under ultra violet irradiation. The experimental results showed the azo red dye was degraded by 76% in 120 minutes when chitosan capped ZnO nanoparticles under ultra violet irradiation were used as removal catalyst, besides removal of colour. Synthesized chitosan capped ZnO nanoparticles exhibit outstanding photocatalytic activity under UV irradiation. A comparative study of photodegradation efficiency among pure ZnO, PVP caped ZnO and chitosan capped ZnO also performed. Metal oxide Semiconductor photocatalysis frequently leads to partial or complete mineralization of organic contaminants.

(Received January 21, 2018; Accepted July 13, 2018)

Keywords: Azo red dye, Chitosan, Organic pollutants, Photodegradation, PVP, ZnO

1. Introduction

Now a day the growing population has led to the increase contamination of river water, ground water and surface in recent years. Organic dyes used in textile manufacturing and food industries are main sources of the environmental pollutions due to their toxicity and non-bio degradability to water sources and carcinogenic effects on human being. Acid red 88, also called Solid Red A, 2-Naphthol Red, Toyo roccelline or Fast Red A, having IUPAC name Sodium 4-(2-hydroxy-1-naphthalenylazo)-naphthalenesulfonate with chemical formula $C_{20}H_{13}N_2NaO_4S$, is a almost black when solid. This dye has been used as dye in the cotton, jute, leather and food colorings preservative. However, Azo dyes make the environment pollution on water source and as well as affect the immune system of human beings and its show cancer and genotoxic. Therefore, it is essential to come across an effective method of contamination water treatment in order to remove this hazardous dye from industrial sewages.

Recently metal oxide nano particles are used for photocatalysis application because of their bandgap energies are sufficient for catalysis. The surface to volume ratio of particles is high and it enhances the photocatalytic activity [1,2]. II-VI group semiconductors have been studied because of their unique functions when compared than other semiconductors and they have been shown photoactive nearby UV region. The uses of natural organic materials in the synthesis of nano particles provide an interface for the charge transfer resulting in the increase of

---

[*] Corresponding author: jeere06@gmail.com

photocatalytic efficiency [3,4,5,6,7]. In addition, photocatalytic activity can be increased when enhance the photo absorption in the visible region through surface modification. Chlorophylls are the most efficient molecules to solve these problems because these molecules can absorb the visible light. Then this high absorption enhances the photocatalytic efficiency when coupling with the inorganic nanoparticles, especially semiconductor nanoparticles hybrid system can harvest much light energy [8, 9, 10, 11, 12, 13, 14]. Therefore, in the present work we have used artificially synthetic polymer poly-vinyl pyrolidone and naturally synthetic chitosan as a capping agent to cover the surface of ZnO nanoparticles.

2. Experimental details

2.1 Materials

All chemicals are AR grade and used as purchased without further purification. Zinc nitrate hexahydrate ($Zn(NO_3)_2.6H_2O$), Sodium hydroxide (NaOH), Poly-vinyl pyrolidone (PVP), Chitosan were used as precursors and double distilled water was used as the solvent. Azo red dye was used for photodegradation study.

2.2. Synthesis of pure ZnO, PVP capped ZnO and Chitosan capped ZnO NPs

Synthesis of ZnO nanoparticles were synthesized by soft chemical method. Synthesis of pure ZnO nanoparticles, precursor solution was prepared. The prepared solution was allowed 24 hours reaction time at room temperature. The resulting white precipitate was purified with double distilled water and dried with air at 100^0 C for three hours. For synthesis of pure ZnO (a), PVP capped ZnO (b) and chitosan capped ZnO (c) nanoparticles, the same procedure was used. The capping solution was added in drops into the precursor solution.

2.3. Photodegradation analysis

For photodegradation analysis, 0.1 M azo red dye was dissolved in 150 ml of double distilled water. Then, each 4 mg NPs samples were dispersed in the 50 ml of dye solution and stirred. The catalytic solutions were placed under UV irradiation for degradation of dye with different irradiation time (0, 30, 60, 90 and 120 minutes). The decomposition effect was measured by UV-absorption measurement. The effect of ultra violet light sources on photodegradation of Azo red dye was carried out with a 30 W (UV-C, 254 nm) mercury lamp (Philips). The distance between dye solution and violet light sources was 25 cm.

2.3. Characterization Techniques

XRD patterns of the prepared samples were recorded using the PANalytical diffractometer model. The surface morphology was observed through SEM micrographs were recorded using Quanta model. The optical absorption spectra recorded using Shimadzu UV-Visible spectrophotometer model and the emission spectra were recorded using the Jasco spectrofluorometer model.

3. Results and discussion

3.1. XRD analysis

The powder X-ray diffraction pattern of (a) ZnO, (b) PVP caped ZnO and (c) chitosan capped ZnO nanoparticles are shown in figure 1. All the obtained diffraction peaks were matched with the corresponding hexagonal wurtzite structure with a space group P63mc of ZnO (JCPDS card No.36-1451).The broadened diffraction peaks indicated the formation of nanosized particles. The average particle size of all the nanoparticles was calculated using Debye Scherrer’s formula.

$$D = 0.9\ \lambda/(\beta \cos\theta) \tag{1}$$

Where, D – the average particle size, λ - incident wavelength of X-ray beam, β - full-width at half-maximum intensity and θ - Bragg's diffraction angle respectively.

The calculated average particle sizes were 20 nm, 18nm and 15 nm for samples a, b and c. The average particle sizes of sample b & sample c were decreased when compared with sample a due to the presence of capping agents. The broad reflection peaks and average particle sizes were confirmed the formation of system [14].

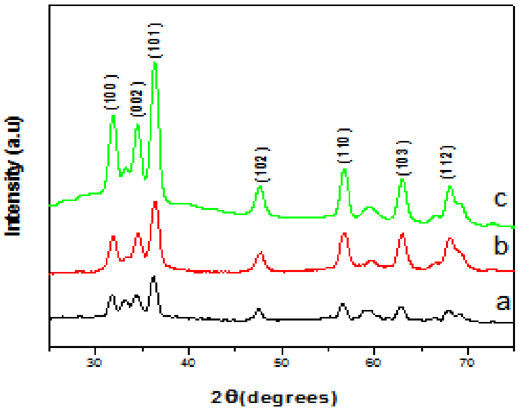

Fig. 1. XRD patterns of (a) ZnO, (b) PVP capped ZnO and (c) chitosan capped ZnO nanoparticles

3.2. Surface analysis

The surface morphology of (a) ZnO and (b) ZnO-PVP are shown in figure 2.The SEM images show that the formed ZnO nano particles were in spherical morphology. The surface agglomeration was observed due to high surface energy of the nanoparticles.

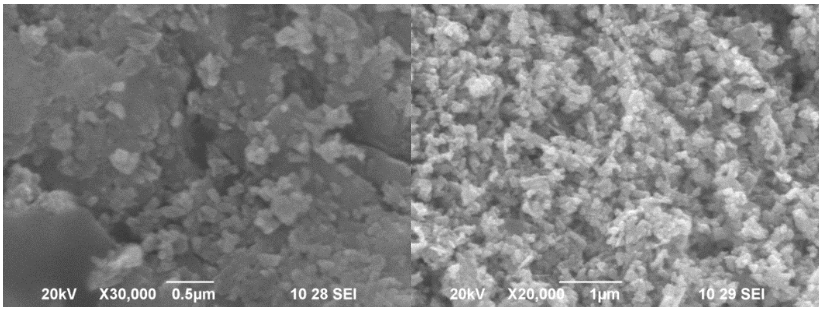

a) *b)*

Fig. 2. SEM micrographs of (a) pure ZnO (b) chitosan capped ZnO NPs

3.3. Optical analysis

The optical absorption spectra all the samples are shown in figure 3. The obtained absorption wavelength of prepared nanoparticles from optical absorption spectra was 335 nm, 336 nm and 338 nm for samples a, b and c respectively. The slight increase in absorption was found with the presence of capping agents. The band gap was calculated using the equation Eg = (hc)/(λ), Where h is Planck's constant, c is the velocity of light and λ is the wavelength of light [14]. The bandgap energy values were 3.72eV, 3.70eV and 3.68eV for samples a, b and c respectively.

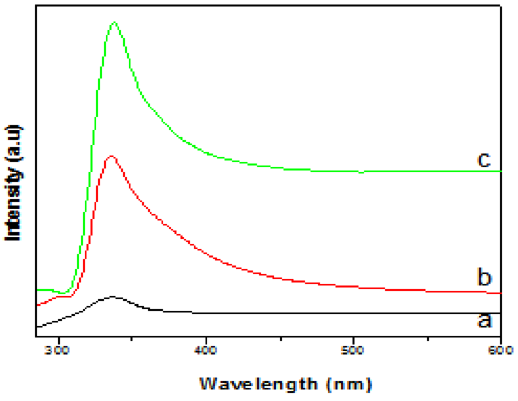

Fig.3. UV optical spectra of (a) ZnO, (b) PVP capped ZnO and (c) chitosan capped ZnO nanoparticles.

The photoluminescence spectra of 4(a) ZnO, 4(b) PVP capped ZnO and 4(c) chitosan capped ZnO nanoparticles are shown in figure 4. A weak excitonic emission and oxygen vacancy related visible emission bands are observed in the ZnO nanoparticles which are maximum at 390 nm and 555 nm, respectively. In the case of polymers capped ZnO nanoparticles, a trap state related blue emission is strong because of the reduced defect/vacancy states in the ZnO crystal. In this case, the chitosan ZnO nanoparticles show a strong and enhanced blue emission which is maximum at 435 nm whereas PVP capped ZnO nanoparticles show different. However, in the both of polymers capped nanoparticles, weak excitonic violet emission also observed. Hence, the emission band position corresponds to ZnO nanoparticles were blue-shifted when compared to bulk ZnO particles and this observed shift is attributed due to the quantum confinement effect [15].

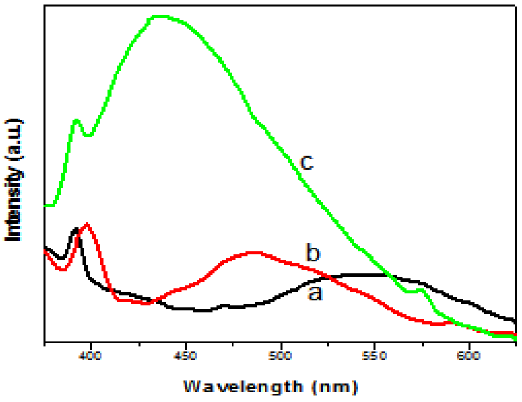

Fig. 4. PL emission spectra of (a) ZnO, (b) PVP capped ZnO and (c) chitosan capped ZnO nanoparticles.

3.4. Photodegradation analysis

The photodegradation spectra of (a) ZnO, (b) PVP capped ZnO and (c) chitosan capped ZnO nanoparticles are shown in figure 5. The UV light was absorbed by ZnO NPs moved the electrons from the valence band (VB) to the conduction band (CB).

The photo generated holes reacted with water and formed hydroxyl radical. The hydroxyl radicals were the most potent oxidizing agents. The degradation rate confirmed the potency of the hydroxyl radical. The photo generated electrons reacted with molecular oxygen and produced superoxide radical anions. These reactive radicals are responsible for the degradation of the azo red dye solution [16].

The hydroxyl radical is an extremely strong, non-selective oxidant that leads to the degradation of organic chemicals:

$$\mathrm{ZnO} + h\nu \rightarrow \mathrm{ZnO}\ (\mathrm{eCB}^{-} + \mathrm{hVB}^{+}) \quad (2)$$

$$\mathrm{hVB}^{+} + \text{dye} \rightarrow \text{oxidation of the dye} \quad (3)$$

$$\mathrm{hVB}^{+} + \mathrm{H_2O} \rightarrow \mathrm{H}^{+} + \bullet\mathrm{OH} \quad (4)$$

$$\mathrm{hVB}^{+} + \mathrm{OH}^{-} \rightarrow \bullet\mathrm{OH} \quad (5)$$

The electron in the conduction band (eCB^{-}) after diffusion to the catalyst surface, can reduce molecular oxygen to superoxide anion. In the presence of organic scavengers, this radical leads to organic peroxides or hydrogen peroxide.

$$\mathrm{eCB}^{-} + \mathrm{O_2} \rightarrow \bullet\mathrm{O_2} \quad (6)$$

$$\bullet\mathrm{O}_{2-} + \text{dye} \rightarrow \text{dye} - \mathrm{OO}\bullet \quad (7)$$

$$\bullet\mathrm{O}_{2-} + \mathrm{HO_2}\bullet + \mathrm{H}^{+} \rightarrow \mathrm{H_2O_2} + \mathrm{O_2} \quad (8)$$

Electrons in the conduction band are also responsible for the production of hydroxyl radicals.

$$\bullet\mathrm{OH} + \text{dye} \rightarrow \text{degradation of the dye} \quad (9)$$

The azo red dye mixed ZnO nanoparticles showed absorption spectra around 500 nm -550 nm and also as the same from dye mixed PVP capped ZnO and chitosan capped ZnO nanoparticles.

The absorption intensity of dye was decreased slowly depends upon the time of UV irradiation which was observed in the visible region and all of the nanoparticles samples shown a good dye degradation effect. Here, the capped ZnO nanoparticles shown increased dye degradation rate than that of pure ZnO nanoparticles. However, the chitosan capped ZnO nanoparticles have shown a higher dye degradation rate and it may be because of the formation of small sized particles and also a higher rate hydroxyl radical formation. It was calculated using the formula,

$$D(\%)=((A_0-A_t)/A_0)\ \mathrm{X}\ 100 \quad (\quad 10)$$

Where, A_0 is the maximum absorption of dye before irradiation and A_t is the maximum absorption of the dye after irradiation [17].

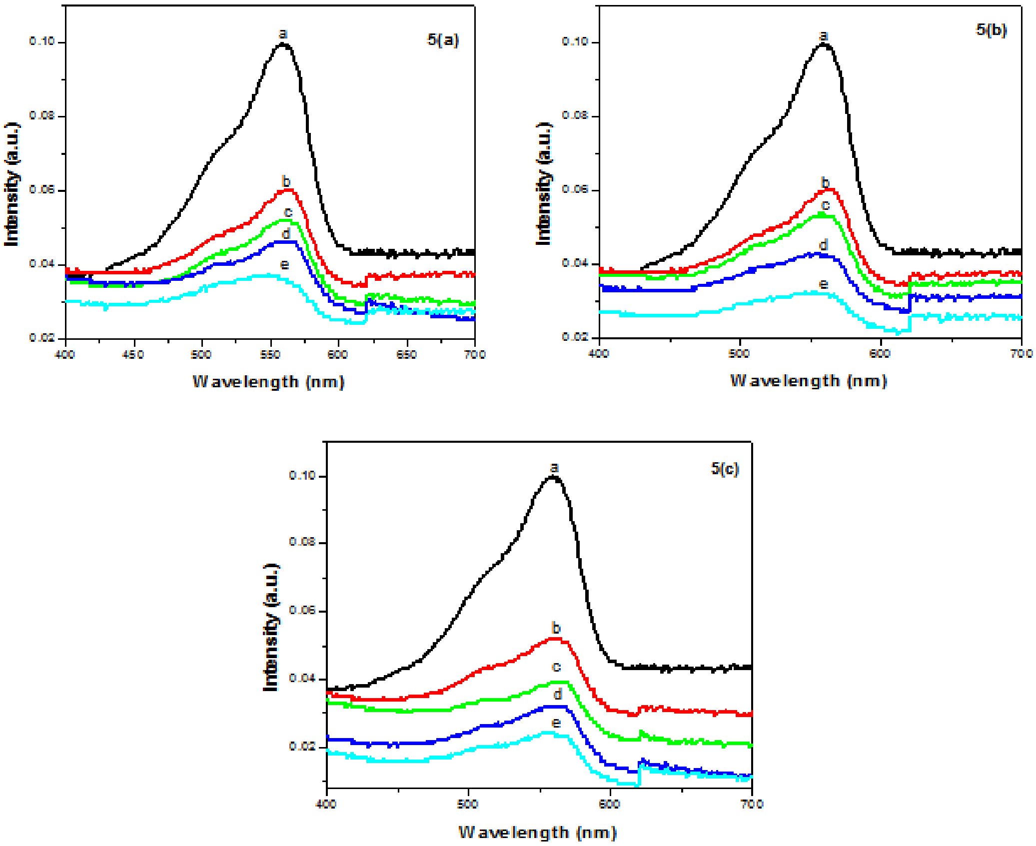

Fig. 5. Photodegradation spectra of (a) ZnO, (b) PVP capped ZnO and (c) chitosan capped ZnO nanoparticles

The dye degradation rate D(%) was estimated at 63%, 67% and 76% for ZnO, PVP capped ZnO and chitosan capped ZnO nanoparticles. Further, the result clearly showed a higher dye removal efficiency of the chitosan capped ZnO nanoparticles. Hence, the observed results conclude that the chitosan capped ZnO nanoparticles was a good dye removal catalyst.

4. Conclusions

The artificial and natural, synthetic polymers of poly-vinyl pyrolidone and chitosan capped ZnO nanoparticles were prepared using the soft chemical method. Their structural and optical properties were analyzed using XRD, SEM, UV and PL techniques. Finally, the photodegradation performances of prepared nanoparticles were investigated using azo red dye.

The dye degradation rate D(%) was estimated as 76% for chitosan capped ZnO-nanoparticles. An enhanced degradation effect was observed from the chitosan capped ZnO nanoparticles against azo red dye. Therefore, we conclude the prepared nanoparticles could be a suitable dye removal catalyst. Especially, the chitosan capped ZnO nanoparticles are potential candidates for dye removal catalyst than the other ZnO nanoparticles.

References

[1] M. R. Hoffmann, S.T. Martin, W. Choi, D.W. Bahnemann, Chemical reviews **95**(1), 69 (1995).

[2] P. Calza, E. Pelizzetti, Pure and Applied Chemistry, **73**(12), 1839 (2001).

[3] T. Sato, K. Masaki, T. Yoshioka, A. Okuwaki, Journal of Chemical Technology and Biotechnology, **58**(4), 315 (1993).
[4] S. Qian, C. Wang, W. Liu, Y. Zhu, W.Yao, X. Lu, Journal of Materials Chemistry **21**(13), 4945 (2011).
[5] V. Rajendran, M. Lehnig, C. M. Niemeyer, Journal of Materials Chemistry **19**(35), 6348 (2009).
[6] H. Li, X. Gui, C. Ji., P. Li., Z. Li, L. Zhang, H. Zhu, Nano Research, **5**(4), 265 (2012).
[7] K. F. Michael, Photochemical & Photobiological Sciences **3**(9), 859 (2004).
[8] M. Joshi, S.P. Kamble, N. K. Labhsetwar, D.V. Parwate, S. S. Rayalu, Journal of Photochemistry and Photobiology A: Chemistry **204**(2), 83 (2009).
[9] S. Mackowski, S. Wörmke, A. J. Maier, T. H. Brotosudarmo, H. Harutyunyan, A. Hartschuh, C. Bräuchle, Nano letters, **8**(2), 558 (2008).
[10] C. Li, F. Wang, C.Y. Jimmy, Energy & Environmental Science, **4**(1), 100 (2011).
[11] G. Gao, Y. Deng, L. D. Kispert, The Journal of Physical Chemistry B, **102**(20), 3897 (1998).
[12] A. O. Govorov, I. Carmeli, Nano letters, **7**(3), 620 (2007).
[13] R. Jiang, H. Zhu., J. Yao., Y. Fu, Y. Guan, Applied Surface Science **258**(8), 3513 (2012).
[14] K. Vidhya, M. Saravanan., G. Bhoopathi., V. P. Devarajan, S. Subanya, Applied Nanoscience, **5**(2), 235 (2015).
[15] D. Sun, H.J. Sue, N. Miyatake, The Journal of Physical Chemistry C, **112**(41), 16002 (2008).
[16] N. Serpone, A.V. Emeline., S. Horikoshi, V. N. Kuznetsov, V. K. Ryabchuk, Photochemical & Photobiological Sciences, **11(7)**, 1121 (2012).
[17] C. Chen, J. Liu., P. Liu and B. Yu, Advances in Chemical Engineering and Science **1**(01), 9 (2011).